Reports

Direct Observation of Dissociated Dislocations in Garnet

F. M. ALLEN, B. K. SMITH, P. R. BUSECK

Dislocation core structures in garnet [grossularite $(Ca_{2.9}Fe^{II}_{0.1})(Al_{1.9}Fe^{III}_{0.1})Si_{3.0}O_{12}$] have been examined with near atomic resolution transmission electron microscopy. Dissociated dislocations have been observed as parallel $a/4\langle 111\rangle$ partial dislocations that are separated by stacking faults. The partial dislocations have narrow cores (~3 burgers vectors), and the stacking fault zone between the narrow partial dislocations is apparently a low-energy configuration that results from the occupancy of previously unfilled dodecahedral and tetrahedral sites. Previous studies of garnet dislocations suggested that dissociation involves departures from garnet stoichiometry (that is, trace amounts of impurities), but evidence of detectable amounts of impurities has not been found even in the highest resolution images. These results have implications for mantle mineral rheology and transformations as well as for ceramics of material science interest.

CRYSTALLOGRAPHIC DEFECTS IN dense oxides greatly influence their mechanical, electrical, and chemical properties, but little is known about the atomic structure of the defects and how defect structures control the diffusibility and concentrations of atoms in the region of the defect. Conventional transmission electron microscopy (TEM) methods have been used to determine the displacement of unit cells on either side of a defect, but these oxide materials have unit cells that contain large numbers of atoms relative to simple ionic solids or metals. A unit cell displacement in some dense oxide structures may involve hundreds of atoms, and it is difficult to derive atomic models for such large structural perturbations.

The garnet structure is common to a number of natural and synthetic oxides and has been studied extensively from both mineralogical and material science perspectives. Synthetic garnets (for example, yttrium iron garnet) are of interest because of their ferrimagnetic properties, and contain well-studied defects that form during growth. Defects in natural silicate garnets are not as well studied, although they are significant in some metamorphic reactions (*1*). Garnet dislocations are topologically similar to those in other high-pressure oxide phases, and the atomic structure of garnet defects is similar to defect structures in other oxides. We report high-resolution TEM (HRTEM) images of dislocations in naturally occurring garnet. These images provide direct evidence that the garnet structure in the immediate vicinity of the dislocations (the dislocation "core") is composed of a region of structural perturbations that involve the occupancy of previously unfilled crystallographic sites.

All garnets have a body-centered cubic unit cell and a chemical formula of $X_3Y_2Z_3O_{12}$. In natural garnets, X and Y are divalent and trivalent cations, respectively, and Z is silicon, whereas X, Y, and Z are generally all trivalent cations in synthetic garnets. The unit cell consists of eight formula units, with cell edges of ~1.2 nm; the exact value depends upon composition. The garnet structure can be most easily visualized with a unit cell of octahedrally coordinated Y cations. The octahedra occupy the corners and centers of each octant of the garnet cell; each octant is slightly distorted relative to its neighbors. An octant can thus be used as a simplification of the larger garnet unit cell (Fig. 1). The X cation is surrounded by eight oxygens in a distorted cube coordination and shares opposite edges with tetrahedrally coordinated Z cations. The opposite edge of the Z tetrahedron defines the edge of the next X distorted cube to produce an X-Z alternation that trends parallel to the cube edges of the garnet unit cell.

Displacement vectors ("burgers vectors") for dislocations can be defined that relate two equivalent points of the lattice so that no closure error is produced after completing an atom-by-atom circuit through the structure around the dislocation. The energy of a dislocation is proportional to the length of its burgers vector, so that dislocations with short burgers vectors are favored during deformation. In garnet, the shortest lattice vectors are $a/2\langle 111\rangle$ and $a\langle 100\rangle$ in Miller index notation (*2*), with lengths of about 0.7 and 1.2 nm, respectively.

Dislocations that displace only subunits of a unit cell are called partial dislocations, and they are separated by a planar region of mismatch, or "stacking fault." Two or more partial dislocations terminate the stacking fault region so that all of the sublattice translations sum to a lattice vector, and thus perfect registry is restored. Stacking fault regions are important sources and sinks for trace interstitial solutes and may serve as preferred regions for second-phase growth (*1*). Dissociation is the splitting of a perfect dislocation into two or more partial dislocations, and the degree of dissociation (that is, the area and type of stacking fault) is an important material parameter in garnet and other complex silicates.

The similarity of the octants in the garnet structure led Rabier *et al.* (*3*) to propose defects in the garnet cell based on the Y octahedra sublattice rather than the larger crystallographic unit cell. Dissociation reactions for garnet that minimize stacking fault energy were then proposed in which the distortions to the octahedral sublattice are minimized. The $a/2\langle 111\rangle$ burgers vector (that is, the body diagonal of the octant in Fig. 1) can thus be split into two $a/4\langle 111\rangle$

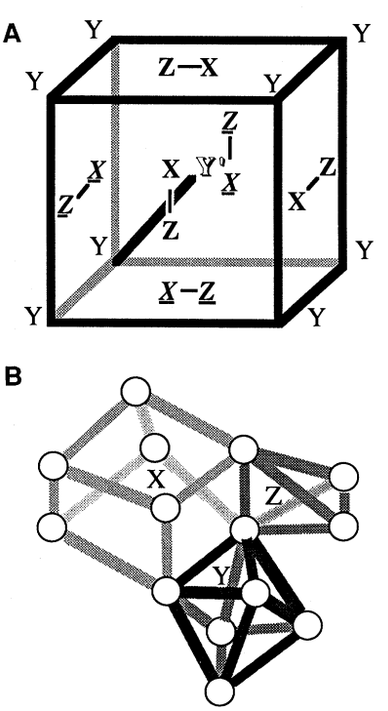

Fig. 1. (**A**) An octant of the garnet unit cell, defined by the octahedral Y sites on the corners of the cube. The arrangement of X and Z sites is also shown. The X and Z sites alternate along the $\langle 100\rangle$ directions. Underlined X and Z sites are on the hidden faces and Y′ is at the center of the cell. (**B**) The polyhedral coordination of X, Y, and Z sites.

F. M. Allen and B. K. Smith, Department of Geology, Arizona State University, Tempe, AZ 85287-1404.
P. R. Buseck, Departments of Geology and Chemistry, Arizona State University, Tempe, AZ 85287-1404.

partial dislocations (the body-centering vector of the octant). Another possible mechanism involves the separation of $a/2\langle 111\rangle$ into $a/2\langle 100\rangle + a/2\langle 011\rangle$ (equal to the sum of a cube edge plus a face diagonal). Finally, for $a\langle 100\rangle$ dislocations, reactions involving pairs of $a/4\langle 111\rangle$, $a/2\langle 001\rangle$, or $a/2\langle 011\rangle$ displacements are also possible.

Although the octahedral distortions are not great for these reactions, the distortions of the X and Z polyhedra differ significantly depending on the mechanism. They can be classified as two types [following (*3*)]: $a/4\langle 111\rangle$ partial dislocations produce faults that fill previously unoccupied sites in the structure, whereas $a/2\langle 001\rangle$ and $a/2\langle 011\rangle$ break the alternation of the X and Z sites but do not fill previously unoccupied sites. Although one might expect that the $a/2\langle 001\rangle$ type of defect is more likely because it requires only a disruption of the ordering of X and Z sites, the $a/4\langle 111\rangle$ type seems to be preferred (*1*).

TEM studies have shown that the $a/4\langle 111\rangle$ dissociation of $a/2\langle 111\rangle$ screw dislocations occurs for synthetic garnets deformed at high temperatures (*4*) and in natural garnets deformed in the presence of dehydrating mineral assemblages (*1*). The $a/2\langle 001\rangle$ type of dissociation mechanism has not been observed. However, dissociation of garnet dislocations is difficult to observe with conventional TEM techniques, and there have been a number of earlier investigations in which dissociation could not be established (*5*).

The separation of partial dislocations to observable widths is hindered in garnet and other complex structures by the high energy of the stacking fault region. Separation of two partial dislocations only occurs where similarities between the faulted and unfaulted structures are small, such as for displacements to nearly equivalent crystallographic sites or small rotations of coordination polyhedra.

The part of the structure disrupted by a dislocation is referred to as the "core" region. For complex oxides that are even slightly distorted by partial dislocations, separation widths may be no larger than several unit cells, essentially equivalent to the core of a nondissociated perfect dislocation. Despite the small widths, advances in HRTEM have made it possible to obtain structure images of dissociated defects in some chain and sheet silicate minerals (*6*).

Two HRTEM images of dissociated dislocations are shown for grossular garnet (*7*) (Figs. 2 and 3). The garnet is optically birefringent and exhibits sector-twinning on the {110} growth surfaces. Thin sections were cut normal to these growth surfaces and revealed stacks of planes that correspond to differently ordered layers of atoms (*8*). Strain results from lattice mismatch across such layers and produces defects at the boundaries. The dislocations were introduced during growth of these crystals; there is no geological evidence that the garnets were plastically deformed at this locality (*7*). Similar grown-in defects in synthetic garnets have been studied by TEM methods (*5*), but there was no unequivocal evidence for dissociation.

The crystallographic orientation and contrast for the defect in Fig. 2A is indicative of a straight dislocation segment parallel to $[1\bar{1}1]$. Closure around the dislocation indicates a burgers vector of $a/2\langle 111\rangle$ for the undissociated segments (lower left and upper right of image). The displacement is parallel to the length of the dislocation such that the segments are screw dislocations. The dissociation of the dislocation produces two parallel segments that are separated by a faulted region. The dissociation reaction is restricted to the $(\bar{1}01)$ plane [inclined to the viewing direction, as shown in accompanying cartoon (Fig. 2C)] and hence is a glissile

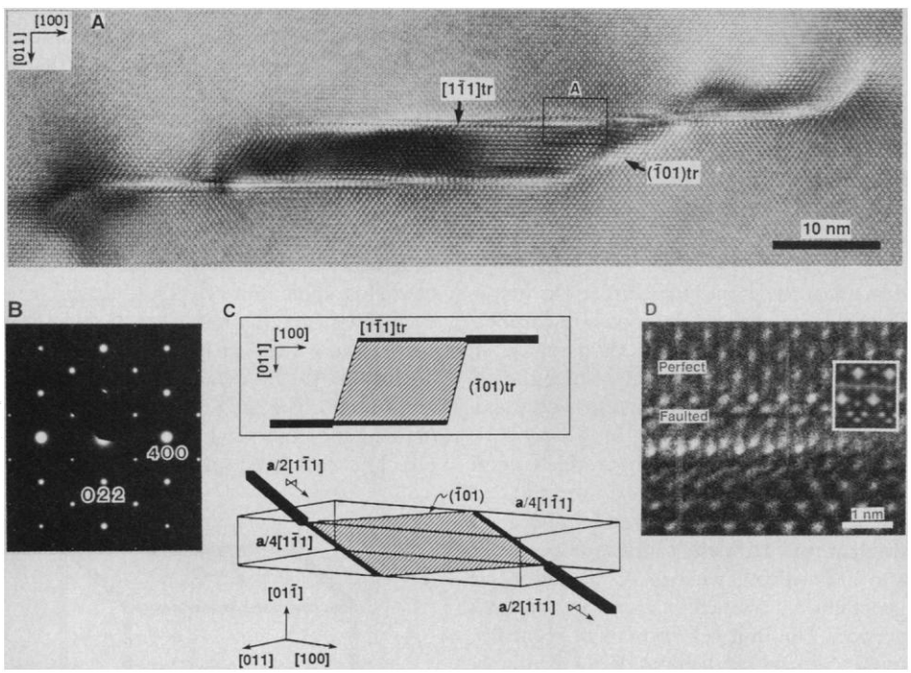

Fig. 2. (**A**) Experimental [0$\bar{1}$1] HRTEM image of a dissociated dislocation in grossular garnet. A selected area electron diffraction pattern is shown for reference in (**B**). Closure of the image around the dislocation (that is, the number of fringes parallel to different crystallographic directions) indicates a burgers vector of $a/2\langle 1\bar{1}1\rangle$ for the undissociated segments [shown as heavy black lines in (**C**)]. In the micrograph (A), this direction is shown in projection (labelled as [1$\bar{1}$1]tr to indicate that this is the trace of the [111] direction). Dissociation produces two parallel $a/4\langle 111\rangle$ partial dislocations separated by a stacking fault (shaded regions in cartoon). The partial dislocations are narrow, with widths of ~3 burgers vectors. The area marked in the black box is magnified in (**D**), in which the experimental and calculated [0$\bar{1}$1] HRTEM images of perfect and faulted grossular garnet are compared. The apparent doubling observed in the experimental image at the stacking fault interface is simulated by filling X and Z voids. The calculated image (inset) is for 104.7-nm thickness and −50-nm defocus.

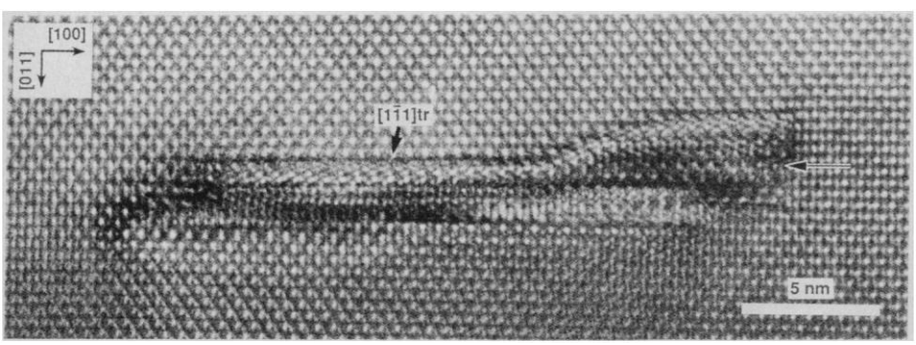

Fig. 3. Experimental [0$\bar{1}$1] HRTEM image of a dissociated dipole in grossular garnet. As in Fig. 2, a dislocation has separated into two $a/4\langle 111\rangle$ partial dislocations, but in this case by a nonconservative process into a dipole. The closure error of the dipole indicates that dissociation entailed loss of a row of unit cell material (arrow).

dissociation (restricted to slip plane) of an $a/2\langle 111\rangle$ dislocation into two parallel $a/4\langle 111\rangle$ partial screw dislocations.

Image simulations (*9*) were done to test whether the modification of the lattice image between the dissociated dislocation segments in Fig. 2A resulted from the occupancy of previously unfilled X and Z sites (*2*). A "doubling" in the image is seen at higher magnification where the faulted and unfaulted structures meet (Fig. 2D). The simulation for a thickness of 104.7 nm at a defocus of −50 nm most closely resembles the experimental images in the unperturbed crystal regions and at the dislocation. The model of filling X and Z voids at the dislocation is consistent with the apparent doubling of the lattice image.

Deviation from garnet stoichiometry (that is, the presence of impurities) in the stacking fault region may be expected to enhance or stabilize the dissociation of the $a/2\langle 111\rangle$ dislocation (*1*). However, no apparent inclusion or other preexisting defect is observed. Three possible explanations for this absence may be that (i) interstitial atoms that may stabilize dissociation are present in low concentrations and are not visible, (ii) atoms with nominally different valence may reside on an existing site (such as Fe(III) on X), which would not otherwise affect the structural image, or (iii) the dislocation has experienced motion after its formation as a growth defect and that the dissociation is glide-induced. The first two possibilities are intriguing because they imply that low quantities of dopant or solute atoms or slight deviations from stoichiometry may lead to dissociation in garnet and potentially in other complex silicates and oxides.

Evidence to support the stabilization of dissociated cores by trace amounts of solute is provided in Fig. 3, in which a grown-in dislocation has dissociated into a dipole of two $a/4\langle 111\rangle$ partial dislocations. However, this dissociation occurred by a nonconservative ("climbing") process, because the closure error of the dipole indicates that dissociation entailed loss of material equivalent to one unit cell (arrow). It is unlikely that these garnets were plastically deformed, so the only mechanism for the formation of this dissociated dipole would be the flux of vacancies to the precursor core segment, which would cause the small but observable dissociation through a Suzuki-type mechanism (*10*).

There are several important problems in mineral physics that are well suited for HRTEM analysis of dislocation cores. For example, the mechanism of the olivine-spinel transformation at 400-km depth in the mantle may depend on the dissociation of olivine defects (*11*). Plastic flow of the lower mantle may be strongly influenced by perovskite defect structures, and inferences have been made that the core regions of dislocations in perovskite are also dissociated (*12*). The crystal structures and electron scattering of olivine and perovskite are similar to garnet; recent reports of the imaging of dissociated olivine defects (*13*) demonstrate that HRTEM analysis of defects in dense oxides may be generally feasible.

REFERENCES AND NOTES

1. B. K. Smith, in *Metamorphic Reactions*, vol. 4 of *Advances in Physical Geochemistry*, A. B. Thompson and D. C. Rubie, Eds. (Springer-Verlag, New York, 1985), pp. 98–117.
2. Burgers vectors are described by their length in terms of the lattice parameter a and the crystallographic orientation in Miller index notation. For garnet, which is cubic, the [111] direction is symmetrically equivalent to eight directions (one per octant of the unit cell); this is indicated by the convention ⟨111⟩ that signifies the group of symmetrically related [111] directions. The group of symmetrically related (hkl) planes is conventionally written as $\{hkl\}$.
3. J. Rabier, P. Veyssiere, T. Grilhe, *Phys. Status Sol. A* **35**, 259 (1976).
4. J. Rabier, P. Veyssiere, H. Garem, *Philos. Mag. A* **44**, 1363 (1981).
5. J. W. Matthews and T. S. Plaskett, *Phys. Status Sol. A* **35**, 577 (1976). R. K. Mishra and G. Thomas, *J. Appl. Phys.* **49**, 1876 (1978).
6. D. R. Veblen, in *Point Defects in Minerals*, vol. 31 of *Geophysical Monographs*, R. N. Schock, Ed. (American Geophysical Union, Washington, DC, 1984), pp. 122–131; _____ and P. R. Buseck, *Am. Mineral.* **65**, 599 (1980).
7. Garnets were single crystals of grossular $[(Ca_{2.9}Fe^{II}_{0.1})(Al_{1.9}Fe^{III}_{0.1})Si_{3.0}O_{12}]$ obtained from Belvedere Mountain near Eden Mills, Vermont. Fieldwork in this area demonstrates that no appreciable plastic deformation has affected these garnets [A. H. Chichester, A. Albee, W. M. Cady, *U.S. Geol. Surv. Prof. Pap.* **1016** (1978)] and our TEM observations did not detect evidence consistent with appreciable plastic deformation (for example, slip plane traces or recovered dislocation frameworks). The HRTEM images of the dislocations were obtained from thick regions (100 to 150 nm) of atom-milled foils of these crystals. The micrographs were taken with a JEOL-4000EX microscope, a 400-keV instrument with a point-to-point resolution of ~0.17 nm. This microscope is equipped with a high-brightness LaB_6 electron gun that enables direct image viewing at electron-optical magnifications of 1×10^6 times without loss of resolution from excessive incident-beam divergence. The objective lens has a spherical aberration coefficient (C_S) of 1.0 ± 0.1 mm, as determined by optical diffractogram analysis.
8. F. M. Allen and P. R. Buseck, *Am. Mineral.*, in press; G. R. Rossman, *Geol. Soc. Am. Abstr. Program* **18**, 525 (1986).
9. Simulations were calculated with the Arizona State University versions of multislice-image simulation programs [K. Ishizuka, *Ultramicroscopy* **5**, 55 (1980); _____ and N. Uyeda, *Acta Cryst. A* **33**, 740 (1977)]. Images were calculated in the $[0\bar{1}1]$ direction for a projected unit cell that was 1.185 nm by 1.675 nm ([100] and [011], respectively). The cell was divided along (011); one-half of the cell consisted of normal grossular garnet structure, with calcium in X, aluminum in Y, and silicon in Z (160 atoms), whereas the other half contained these atoms plus calcium and silicon atoms that were displaced by $a/4\langle 111\rangle$ (208 atoms), that represent the stuffed holes at the stacking fault interface. The entire cell was divided along $[0\bar{1}1]$ into eight slices, each 0.209 nm thick, and a phase grating was calculated for each slice. Five hundred slices were integrated to yield a total thickness of 104.7 nm; a propagation function was applied between the slices. Diffracted waves (4096) were used in the potential distribution and phase-grating calculations with a $(\sin\theta)/\lambda$ limit of 30 nm^{-1}. Spherical aberration, voltage, beam divergence, and defocus spread were fixed at 1.0 mm, 400 kV, 0.8 mrad, and 10 nm, respectively, corresponding to the JEOL-4000EX instrument. A maximum resolution of 0.17 nm was assumed; the effects of beam tilt and crystal tilt were not considered. Calculations were stored for thicknesses of 5.23 nm (every 25 slices) up to 104.7 nm and for defocus values between ~10 nm to ~100 nm in increments of ~5 nm.
10. P. Veyssiere, J. Rabier, H. Garem, J. Grilhe, *Philos. Mag. A* **38**, 61 (1978).
11. H. W. Green II, *Geophys. Res. Lett.* **11**, 817 (1984).
12. J. P. Poirier, J. Peyronneau, J. Y. Gesland, G. Brebec, *Phys. Earth Planet. Inter.* **32**, 273 (1983).
13. M. Kitamura *et al.*, *Nature (London)* **328**, 143 (1987).

14. Work supported by NSF grants EAR-8408168 (P.R.B.), EAR-8517548 (B.K.S.), and DMR-8306501 (ASU Facility for HREM).

6 July 1987; accepted 17 September 1987

Horizontal Plate Motion: A Key Allocyclic Factor in the Evolution of the Great Barrier Reef

P. J. DAVIES, P. A. SYMONDS, D. A. FEARY, C. J. PIGRAM

The Great Barrier Reef complex of northeastern Australia thins dramatically and becomes younger from north to south. These variations are a consequence of the Cenozoic northward movement of the Indian-Australian plate. The temperate climatic conditions that applied off northeast Australia during the early Tertiary were progressively replaced by tropical conditions. The present-day south-to-north facies distribution along the eastern Australian continental margin mimics the Cenozoic vertical facies sequence through the northern part of the Great Barrier Reef region.

THE GREAT BARRIER REEF OF northeastern Australia, which is comprised of approximately 2500 individual reefs and extends for ~2000 km from 9° to 24°S, is the largest reef province on the earth (Fig. 1). Studies in the past 10 years (*1–3*) have defined the major autocyclic factors that affect reef growth. From these results a model has been constructed in

Bureau of Mineral Resources, General Post Office Box 378, Canberra 2601, Australia.